Construction and Building Materials 30 (2012) 439–446

Contents lists available at SciVerse ScienceDirect

Construction and Building Materials

journal homepage: www.elsevier.com/locate/conbuildmat

Characterization of historical lime plasters by combined non-destructive and destructive tests: The case of the sgraffito in Bożnów (SW Poland)

Wojciech Bartz [a,*], Jaroslaw Rogóż [b], Robert Rogal [b], Adam Cupa [b], Pawel Szroeder [c]

[a] Institute of Geological Sciences, University of Wrocław, ul. Cybulskiego 30, 50-205 Wrocław, Poland
[b] Institute for the Study, Restoration and Conservation of Culture Heritage, Nicholaus Copernicus University, ul. Sienkiewicza 30/32, 87-100 Toruń, Poland
[c] Institute of Physics, Nicholaus Copernicus University, ul. Grudziądzka 5/7, 87-100 Toruń, Poland

ARTICLE INFO

Article history:
Received 14 September 2011
Received in revised form 16 November 2011
Accepted 2 December 2011
Available online 3 January 2012

Keywords:
Historic plaster
Sgraffito
Characterization
Non-destructive tests
Destructive tests

ABSTRACT

Mortars used in the two-color sgraffito, dated back to 17th century, have been investigated in order to fully characterize the material and to evaluate the state of its preservation. The non-destructive tests carried out "in situ", comprising thermal imaging and ground penetrating radar, revealed the inner structure of the decoration, which was exfoliated from the wall in ca. 90%. The obtained thermograms and the GPR scans allowed to choose sampling areas for subsequent destructive-tests, performed by means of optical microscopy, chemical analysis, granulometric analysis, X-ray diffractometry, scanning electron microscopy, infrared spectroscopy and differential thermal/thermogravimetric analysis. The results reveal the decoration is composed of two separate coats of lime plasters: (1) the primer plaster and (2) the sgraffito plaster. Both the coats appeared to be a mixture of lime binder (aerial lime) and fine- to medium-grained sand, with addition of small amounts of brick chunks and charcoal. The latter is abundant in the sgraffito plaster, serving as a coloring agent. For elimination of plasters exfoliation, a calcareous PLM-A product of C.T.S. Italy was applied by injection. The non-destructive studies performed after this conservation demonstrates that the rehabilitation work has reestablished homogeneous structure of the sgraffito decoration.

Our study indicates that full characterization and proper reconstruction of ancient mortars could be attained by complementary employment of destructive and non-destructive test methods. Moreover, repetition of the non-destructive tests after the rehabilitation works provide valuable insights into their effectiveness.

1. Introduction

The analytical characterization of the historical sgraffito decorations can provide a set of data that is vital when defining conservation strategies, as it provides information about the technology of historical mortars, their composition and the degree of weathering. From the recently developed scheme of examinations, the information about filler, binder, and porosity of mortars can be revealed, as well as materials introduced during the conservation treatments and atmospheric pollutants condensed inside the pores. Changes in mineralogical composition of mortars can highlight the proper consolidation methods during the planned conservation treatment.

The aim of this work is to study and to characterize the ancient mortars used in the two-color sgraffito decoration (Fig. 1). It is located on the northern wall of the western tower of the church in Bożnów, a small village situated in SW Poland. The sgraffito was completed by Christoph Rutsch and his two assistants in 1609. White lime plaster (the primer plaster) was covered with a layer of a lime colored gray with charcoal (the sgraffito plaster), where the ornaments were scraped off.

In the 19th century the sgraffito was covered with a layer of plaster. In 1931 the decoration was uncovered by German scholars. However, due to the poor state of preservation the decoration was plastered up. In 1972 the sgraffito was uncovered again and subjected to restoration treatment (Fig. 1a and b). For over 30 years the object was exposed to rainwater that trickling from the tower roof, washed out the lime paint and brought about delamination and huge plaster losses (Fig. 1c). The capillary rise of water as well as the change of temperature and humidity conditions were also responsible for the deterioration.

For elimination of plasters exfoliation, in 2008 after detailed examination a calcareous PLM-A product of C.T.S. Italy was applied by injection. This material provides joints permeable for gas and vapor and shows porosity, water absorption and hygroscopic properties similar to those of the original sgraffito from Bożnów. It is resistant to temperature and humidity changes characteristic of the climate in Poland. The current condition of the sgraffito, after complete restoration in 2008, is shown in Fig. 1d.

* Corresponding author. Tel.: +48 71 3759205; fax: +48 71 3759371.
E-mail address: wojciech.bartz@ing.uni.wroc.pl (W. Bartz).

0950-0618/$ - see front matter © 2011 Elsevier Ltd. All rights reserved.
doi:10.1016/j.conbuildmat.2011.12.045

Fig. 1. The 17th century sgraffito decoration from the church in Bożnów (SW Poland). State of preservation before (a) and after conservation treatment in 1972 (b). State of preservation before (c) and after conservation treatment in 2008 (d).

In order to sufficiently characterize the sgraffito decoration and subsequently to design the repair mortar, a basic schema of the experimental methods proposed by Arıoglu and Acun [1] was applied. Destructive test methods (requiring sampling of the object i.e. petrographical and mineralogical analyses) were preceded by non-destructive test methods, carried out "in situ". In our particular case, the non-destructive tests comprised Infrared Thermography (IT), and ground penetrating radar (GPR). The former has been widely used for the non-destructive analysis of historic art and architecture, where it has been applied to identify and to map structural defects and the presence or movement of moisture through bulk historical materials (walls, plasters, masonry). Recent advances in infrared technology have led to the development of new applications which facilitate monitoring of the art conservator treatment of wall decorations such as frescos [2,3]. David and Daniels [4] have shown that GPR can be employed successfully in near surface studies, therefore the infrared imaging was supplemented by the three-dimensional ground penetrating radar (3D GPR) which was applied for prospecting voids.

2. Experimental methods

Thermal imaging (IT) was performed using infrared camera Therma-CAM™P65. The images were recorded in the range of wavelength 7.5–14.0 μm. The emissivity of the object was fitted to 0.90. The images was performed at relative humidity of 40% and at ambient temperature 25 °C and 20 °C before and after conservation treatment, respectively. The distance between the camera and the object was fitted to 7 m. GPR profiles were recorded using IDS RIS 2K "ALADDIN SK2" system equipped with 2 GHz bipolar antenna.

The area of sampling was chosen on the basis of non-destructive examinations, that fully revealed inner structure of decoration. Representative samples of the primer plaster and the sgraffito plaster, weighing ca. 60–80 g, were taken with the use of hammer and chisel for subsequent investigations. For spectroscopic analyses the samples of the mass of several mg were carefully scratched off directly from the decoration.

Following the scheme of analytical procedure for destructive tests proposed by Middendorf et al. [5], optical microscopy (OM) a preliminary approach for the qualitative characterization of the examined mortars. First, samples were dried to remove moisture at the temperature below 40 °C to avoid forming microcracks and to restrict dehydration of possible hydrous minerals [6]. After impregnation with low-viscous resin under vacuum, thin sections were prepared by grinding and polishing with paraffin/silicon-carbide suspension, to attain thickness of 30 μm. Optical observation of thin sections was done using a polarizing microscope.

For the chemical analysis, two representative samples were crushed in an agate mortar and dried until constant weight. Subsequently, 1 g of the sample was digested with hot HCl (2 M), following the procedure proposed by Alvarez and co-authors [7] and the soluble fraction was analyzed. According to RILEM procedure [5] the contents of Al, Mg, Fe, Na, K, and Ca were determined by Atomic Absorption Spectroscopy (Avanta Sigma GBC, in the Laboratory of Soil, at the Institute of Geography and Regional Development of the University of Wrocław, Poland). The content of acid soluble SiO_2 was determined using Atomic Emission Spectroscopy (Varian 700 ES, in DM Laboratory of Environmental Analyses in Siechnice, Poland).

Microstructures, crystals morphology and their composition were studied by means of scanning electron microscopy (SEM), with energy dispersive X-ray analysis (EDX). Freshly broken samples were covered with a thin carbon layer under vacuum conditions and studied with HITACHI S-4700 microscope at accelerating voltage of 20 kV, in Laboratory of Field Emission Scanning Electron Microscopy and Microanalysis at the Institute of Geological Sciences of the Jagiellonian University.

Next step in our approach was sieve analysis, carried out in order to evaluate grain size distribution, as well as to obtain separated material for subsequent instrumental analysis. Samples were ground in an ultrasonic cleaner for ca. 1.5 h, dried at 40 °C and carefully weighted. Afterwards the granulometric analysis of the samples was performed by mechanical sieving with ISO 565 series sieves, and sieve interval of 1Φ, starting with sieve size of 0Φ (1.0 mm) and end sieve size of 4Φ (0.063 mm). According to numerous authors [8–10] the finest fraction <0.063 mm should be considered as strongly enriched in binder, however insignificant quantities of the filler could be found within this particle size range [9]. Next, separated samples on binder and filler were analyzed independently.

For mineralogical characterization of binder as well as filler, X-ray powder diffraction method (XRD) was applied using Siemens D 5005 powder diffractometer (at the Institute of Geological Sciences, University of Wrocław, Poland), CoKα radiation, scanning speed 2Θ = 2.0 deg./min (fraction >0.063 mm) and 2Θ = 1.0 deg./min (fraction <0.063 mm), 30 kV and 20 mA current, and Diffract—EVA software.

Infrared spectroscopy (IR) was used for gathering qualitative information on some main compounds contained in mortars and for determining the presence of organic compounds as well as colorants. Infrared spectra were recorded at the Institute of Physics, Nicholaus Copernicus University in Toruń, using a Specord M-80 apparatus with a spectral resolution of 2 cm^{-1}. Powdered samples of plaster were run as pressed KBr pellets. The identification of the organic components was achieved using databases found in literature [11].

Apart from optical microscopy, X-ray powder diffraction and IR, thermal studies are complementary techniques, providing a complete characterization of phases constituting mortars [12]. This method allows to identify phases of low crystalinity, which could not be analyzed by means of X-ray diffraction methods. Additionally, results obtained can provide information on the degree of hydration and carbonation for lime based mortars [12]. Therefore, thermal transformation of powdered fraction <0.063 mm, separated from each sample, weighting approximately 300 mg, was recorded with a Derivatograph MOM Q-1500D (at the Institute of Geological Sciences, University of Wrocław). For differential thermal/thermogravimetric analysis (DTA/TG/DTG) samples contained in ceramic crucible were heated at the constant rate of 10 °C/min in static air atmosphere, from room temperature up to 1000 °C.

3. Results and discussion

3.1. Thermal imaging and ground penetrating radar

Thermal images taken from the sgraffito decoration before and after conservation are shown in Fig. 2. A diversified temperature distribution in areas with near surface anomalies is observed (Fig. 2a). The dark area reflects the presence of cement-calcareous screeds, whereas the primer plasters are distinguished by slightly higher temperature. A vast area of plaster exfoliation characterized by higher temperature is recognized as bright fields. Such anomalies are recorded within ca. 80–90% of the plaster preserved. The images obtained after completion of the planned non-destructive and destructive tests and the conservation treatment with PLM-A product (Fig. 2b) are thermally homogeneous proving the efficiency of plaster consolidation during the conservation phase.

The GPR examination (Fig. 3) shows the intersections of pseudo 3D display obtained merging scan acquired with the bipolar 2 GHz antenna. The light fields reflect the area characterized by high amplitude of the radar echo on the anomaly surface. The nearly black areas, in turn, are characterized by small echo amplitude present inside anomalies. The most common anomalies in the examined plaster are voids which result from plaster exfoliation processes. Exfoliation between the wall and the primer plaster, between the

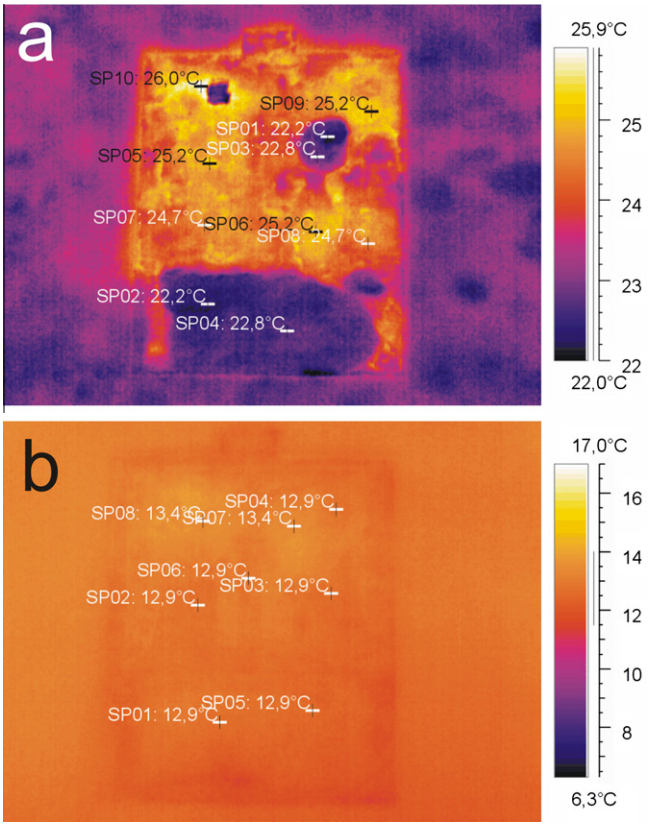

Fig. 2. Infrared images of the decoration before (a) and after conservation treatment (b).

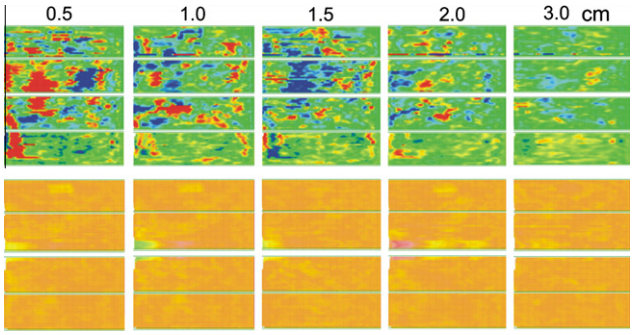

Fig. 3. Intersections of pseudo 3D GPR display of the sgraffito decoration before (upper series of images) and after conservation treatment (bottom series). Above, the depth of intersection is depicted.

primer plaster and the sgraffito plaster and within the inner parts of plasters itself is noticed. As in case of thermal imaging, one of the aims of the GPR study was to assess the efficiency of plaster consolidation. The 3D display shows no anomalies proving the proper plaster consolidation (Fig. 3).

3.2. Optical and electron microscopy

All mortars observed by optical microscopy consist of fine- to medium-grained inert filler, composed of rounded, subrounded to less common subangular grains, generally varied in size and mineralogy, embedded in the very fine-grained matrix (Fig. 4). Quartz plus feldspars (alkali feldspar as well as plagioclases) dominate, whereas uncommon lithic grains (magmatic rocks: granitoids and ryolites) accompany them. The accessory minerals are

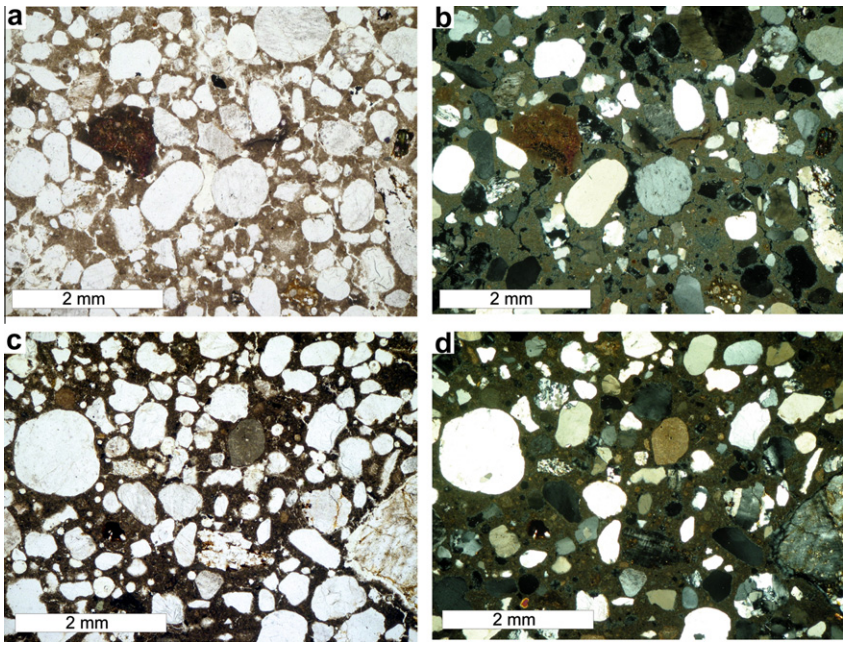

Fig. 4. Microphotograph of the primer plaster (a and b) and the sgraffito plaster (c and d) taken in plane-polarized light (a and c) and cross-polarized light (b and d).

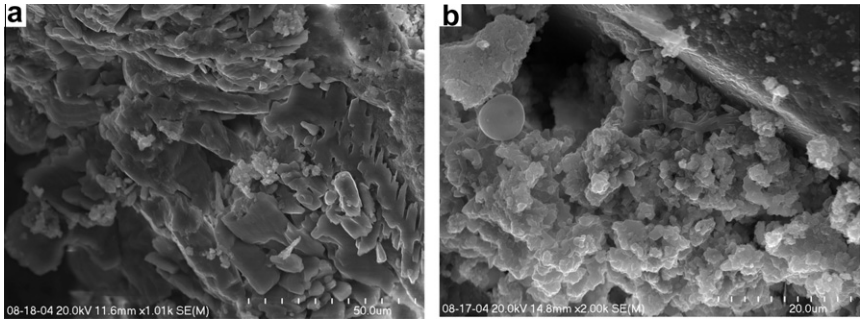

Fig. 5. SEM images of investigated mortars. (a) Large, porous chunk o charcoal (in the center) and micritic binder (upper-right corner), the sgraffito plaster and (b) porous micritic binder (in the center) and grain of the quartz (upper-right corner), the primer plaster.

represented by biotite, amphibole, zircon, with very sparse pyroxene and staurolite. They are associated with sporadic brick and charcoal (chunks as well as superfine dust). The plasters differ by the abundance of the latter. Regarding the primer plaster, there are only traces of the charcoal chunks, which presumably represent remnants of the kiln fuel, whereas the sgraffito plaster contains large quantities: chunks, as well as the charcoal dust (Figs. 4c and d and 5a), serving as a coloring agent [6].

Calcitic matrix is observed at the polarizing microscope (Fig. 4), thus categorizing both mortars as typical lime mortars. It appears as brown micrite in plane-polarized light, medium-coherent with numerous randomly oriented cracks, usually considered as the effect of shrinkage [6]. SEM observations (Fig. 5b) revealed its good adherence to grains of the filler, as well as calcite crystals with different morphologies. Fig. 6a shows coexistence of porous micrite, composed mainly of calcium carbonate with traces of Si and Mg, and locally newly formed euhedral and almost pure crystals of sparry calcite. Moreover, sparse pores are coated with microcrystals of calcite, oriented perpendicularly to the surface. These phenomena indicate solution and re-precipitation of carbonates (so-called autogeneous healing, [6]). Very sparse irregular aggregates of gypsum plates, identified by means of SEM/EDAX (Fig. 6b) occur within the sgraffito plaster only. It is well known that gypsum is the main weathering product of carbonate-based materials, resulting from chemical reaction between calcite and atmospheric sulfur dioxide [13,14]. Its presence is presumably connected to weathering of the outer layer of the sgraffito, exposed to pollution, rather than original binder constituent.

Typically, calcitic matrix of both samples contains sparse, rounded lime-lumps, reaching up to 4.0 mm in diameter. These binder related particles are composed of dark brown micrite (Fig. 4a), free from grains of the filler. SEM/EDX investigations showed they are composed mainly of calcium, with traces of magnesium and silicon. According to the literature data [15–18], the type of lime could be identified on the basis of lime-lumps composition. Apart from the fact that their origin is still under debate [6], we presume that they represent burnt lime chunks, not fully slaked due to water deficiency [19,20]. This suggests that relatively low water/burnt lime ratios were used during slaking, or excess of the water was rapidly added to the lime-pit, generating the impermeable hydrated surface, leaving its interior not fully reacted [21]. The lime-lumps could also come from very short seasoning of slaking lime.

3.3. Chemical analysis

Calcium oxide is the main component of this fraction, whereas the concentration of magnesium oxide as well as R_2O_3 oxides and acid soluble silica are relatively low (Table 1). These compounds

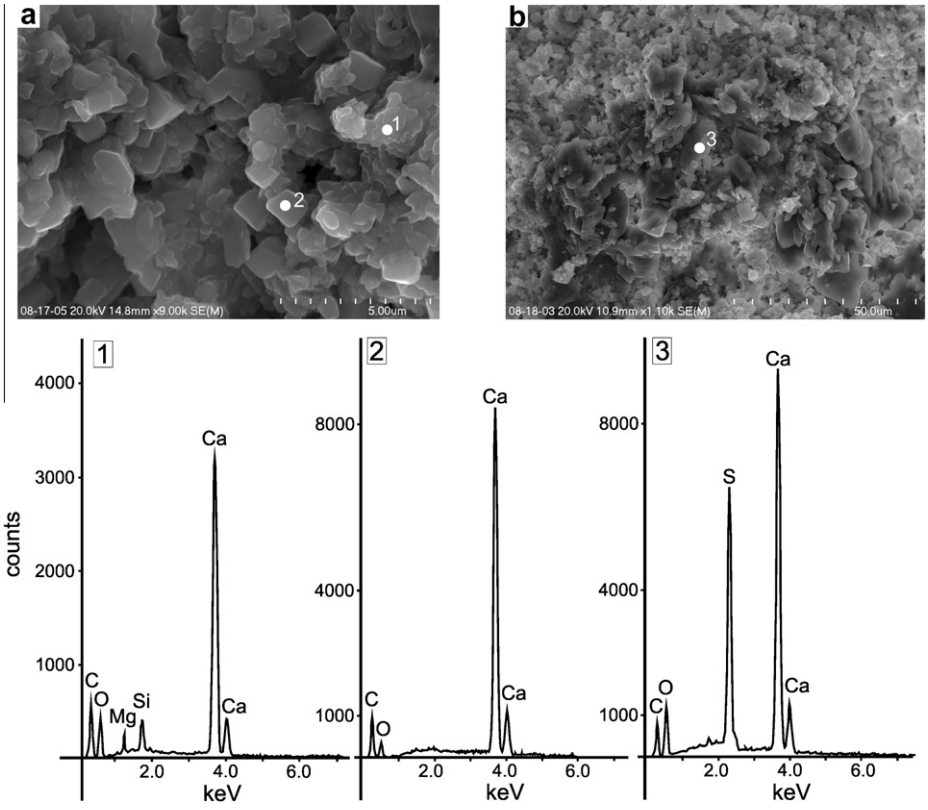

Fig. 6. SEM images of investigated mortars and representative EDS spectra. (a) Neoformed sparry calcite embedded within micritic calcite (the primer plaster) and (b) gypsum aggregate (in the center, the sgraffito plaster).

determine the hydraulic properties of mortar, particularly the acid soluble silica. On the basis of the oxides concentration the Cementation Index (CI) was calculated (Table 1, [22]). Since the values are less than 0.3, mortar from the primer plaster and from the sgraffito plaster is non-hydraulic (Table 1), containing aerial lime as binder. Low concentrations of potassium and sodium (Table 1) indicate low amount of soluble salts.

3.4. Grain size distribution

The granulometric analysis shows that both samples exhibit similar bimodal grain size trends (Fig. 7). The most abundant fraction is below 0.063 mm, with the content of 35 and 39 wt.% for the primer plaster (sample ZW0817) and the sgraffito plaster (sample ZW0818), respectively. Contrarily, the next fraction range (0.125–0.063 mm) shows the lowest value, not exceeding 1 wt.%. Grains with size between 0.250 and 0.125 mm make 5 or 7 wt.% of the total sample. A maximum is defined for coarser grained fraction, i.e. 0.50–0.25 mm, representing up to 22–23% of the total weight. Subsequently, the distributions tend to lesser values, with fraction 1.0–0.5 mm making up 20–18% of the total weight. The coarse-grained material retained by the 1.000 mm sieve exhibits relatively low percentages, ranging between 13 and 17 wt.%.

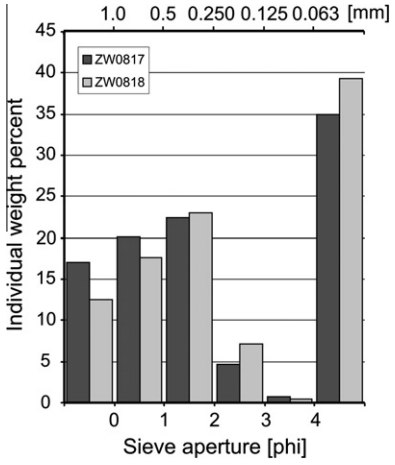

Fig. 7. Grain size distribution of analyzed samples. Sample ZW0817 – the primer plaster, sample ZW0818 – the sgraffito plaster.

On the basis of grain size distribution, the binder/filler ratio per weight was calculated by dividing the mass of sample passing through the sieve 0.063 mm, considered as a binder, and retained

Table 1
Chemical analysis of the acid soluble fraction. Sample ZW0817 – the primer layer, ZW0818 – the sgraffito layer.

Sample	SiO_2[a] (%)	Al_2O_3 (%)	MgO (%)	Fe_2O_3 (%)	Na_2O (%)	K_2O (%)	CaO (%)	CI
ZW0817	0.480	0.101	1.084	1.524	0.038	0.014	21.486	0.110
ZW0818	0.354	0.186	1.731	0.582	0.030	0.026	20.925	0.069

CI = Cementation Index (0.3 < CI < 0.5 = weakly hydraulic, 0.5 < CI < 0.7 = moderately hydraulic, 0.7 < CI < 1.1 = highly hydraulic).
[a] The percentage refers to acid soluble silica.

by the same sieve, considered as a filler. The obtained ratios were found comparable, close to 1:2 for the primer plaster, and 1:1.5 for the sgraffito plaster.

3.5. XRD analysis

XRD powder patterns show that calcite and quartz are the main components in all samples. Quartz coming from filler predominates in XRD patterns for coarser-grained fraction, with less prominent diffraction patterns for K-feldspars (microcline and orthoclase) and plagioclases (albite–anorthite) as accessory minerals (Fig. 8). Calcite predominates in XRD patterns for finer particle size fraction (<0.063 mm) and comes from carbonated lime. Peaks of siliceous minerals are visible, which must originate from filler, passing through sieve 0.063 mm (Fig. 9). The magnesium calcite possibly occurs, but its X-ray pattern overlaps with that of calcite. Its occurrence is supported by the chemical data, revealing presence of magnesium within acid soluble fraction, as well as TGA–DTA results as later will be considered. Identification of the above mentioned constituents confirms the presence of lime base and siliceous filler for both samples. Biotite (d = 9.940, 3.651) or hydrobiotite (d = 10.000, 39.926) are common in all samples (Figs. 8 and 9), whereas tobermorite 9 Å identified by peak for d = 9.375 was found in the sgraffito plaster (sample ZW0818) only (Fig. 9). The presence of the latter is not fully documented, since due to its low concentration most intense peaks (d = 3.028, 3.001) are obscured by those of more abundant phases.

3.6. Infrared spectroscopy

The infrared spectra of the primer plaster and the sgraffito plaster (Fig. 10a and b) show the main calcium carbonate bands at ca. 715, 875, 1425, 1800, 2520, and 2875 cm^{-1}. In the primer plaster the wave number bands at around 1025–1050 cm^{-1} are assigned to starch (Fig. 10a). In spectrum from the sgraffito plaster (Fig. 10b), a well pronounced band at 790 cm^{-1} and a slightly diffuse band at around 1075 cm^{-1} are characteristic to polyvinyl acetate co-polymer with acryl esters. These absorption peaks prove the usage of the Osacryl (Chemical Factory "Oświęcim") during the consolidation of the decoration in 1972. Detection of the Osacryl exclusively within the sgraffito plaster proves its shallow penetration into the decoration. Additionally, the IR spectrum of the sgraffito plaster (Fig. 10b) shows a characteristic band at 3410 cm^{-1} due to the free hydroxyl ions of water.

Typically, the Si–O stretching vibrations marked as bands at 1030 cm^{-1} and 450 cm^{-1} imply the presence of silicates, in our particular case quartz detected by means of optical microscopy and XRD. The lack of these bands on obtained spectra (Fig. 10) arises from a twofold reason: (i) strong bands of polyvinyl acetate co-polymer and starch obscure those of quartz and (ii) during preparation of KBr pellets, larger grains of quartz were separated by hand-picking.

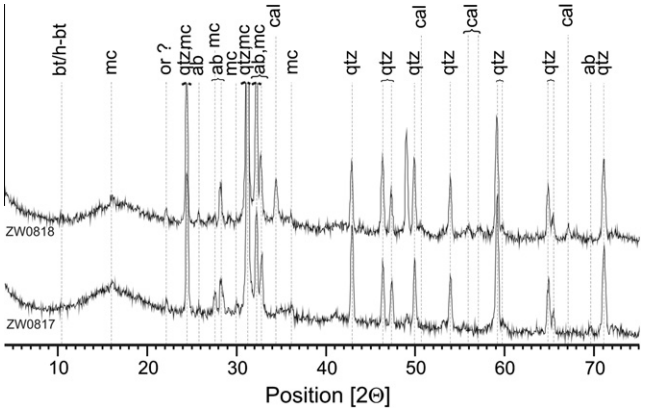

Fig. 8. XRD pattern of particle size fraction >0.063 mm from the primer plaster (sample ZW0817) and the sgraffito plaster (sample ZW0818). Qtz – quartz, mc – microcline, or – orthoclase, bt/h-bt – biotite/hydrobiotite, ab – albite, cal – calcite.

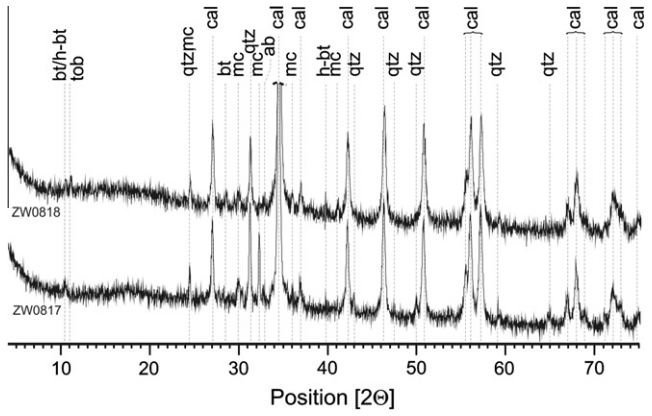

Fig. 9. XRD pattern of particle size fraction <0.063 mm from the primer plaster (sample ZW0817) and the sgraffito plaster (sample ZW0818). Qtz – quartz, mc – microcline, bt/h-bt – biotite/hydrobiotite, ab – albite, cal – calcite, tob-tobermorite.

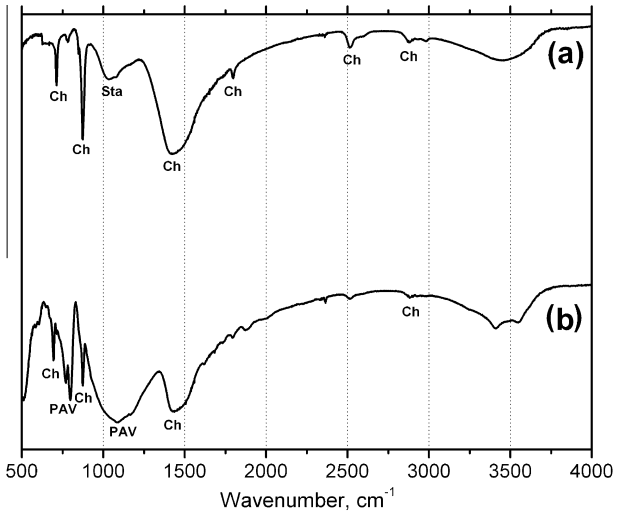

Fig. 10. Infrared spectra of the primer layer (a) and the sgraffito plaster (b). The peaks of calcium carbonate are indicated as 'Ch', starch as 'Sta' and polyvinyl acetate as 'PAV'.

3.7. Thermal analysis

Mertens et al. [23] noticed that the boundaries between thermal events which occur in mortars during controlled heating are strictly arbitrary. This makes it difficult to compare the results of thermal analysis given by various authors. Therefore, we decided to apply commonly used temperature ranges (Table 2), which would best document thermal behavior of wide spectrum of ancient mortars. The first temperature range (below 120 °C) typically corresponds to weight loss due to the release of hygroscopic water [12]. The loss of water of hydrated salts (first of all from gypsum) occurs within temperature range 120–200 °C, whereas the loss of chemically bound water (hydraulic water) is observed between 200 and 600 °C. Finally, temperature above 600 °C causes decomposition of carbonates. Determination of relative weight losses allows to characterize materials, particularly according to their hydraulicity [12].

Table 2
TG-DTG weight losses as a function of the temperature ranges (wt.%).

Sample	<120 °C	120–200 °C	200–600 °C	>600 °C	Total
ZW0817	0.9	1.1	6.3	29.2	37.5
ZW0818	1.1	1.0	5.0	32.0	39.1

The TG/DTG/DTA patterns of both samples exhibit significant endothermic peak occurring in the region of 900 °C, associated with a major weight loss with well visible effect starting from approximately 700 °C, marked on TG/DTG curve (Figs. 11 and 12). This effect is related to dissociation of calcium carbonate, whose amount is estimated to be ca. 67% and 73% of the total weight of samples ZW0817 (the primer plaster) and ZW0818 (the sgraffito plaster), respectively. Marques et al. [24] suggest that such wide temperature decomposition interval, extended up to 950 °C, is indicative of the presence of recarbonated lime, additionally containing calcareous aggregate. However, the OM observations do not confirm the presence of the latter one, nor do they confirm the presence of the underburnt relics of limestone, used for the production of lime. Since the temperature of decomposition of calcium carbonate depends on crystal size, this suggests that at least part of the binder is perfectly crystallized. However, continuous decomposition of carbonates without steps suggests absence of sharply defined different degrees of crystallinity in the micrite [25].

DTA analysis shows a broad exothermic peak, connected with a relatively small weight loss from about 200 to 550 °C (Figs. 11 and 12), which could be attributed to combustion of organic substances [26]. Typically, hydraulic water is also released within this temperature range, but occurrence of hydraulic phases is doubtful since chemical analysis revealed the non-hydraulic character of the investigated mortars. Moreover, despite abundant organic substance (charcoal) detected within sample ZW0818 by means of OM and SEM, both layers of graffito were subjected to preservation with the use of starch, detected by means of infrared spectroscopy. Combination of these two factors provides observed exothermic effect.

The DTA analysis of both samples shows an additional endothermic peak approximately marked at 570 °C, with no corresponding weight changes, which corresponds to the $\alpha \rightarrow \beta$ quartz transformation (Figs. 11 and 12). Although the sieve fraction below 0.063 mm is considered as a binder, finest filler grains, in this particular case quartz, could be detected [10].

A weak endothermic peak occurs at 690 °C (sample ZW0817, the primer plaster). This peak also occurs with sample ZW0818 (the sgraffito plaster), but to a lesser extent (Figs. 11 and 12). It could correspond to first endotherm for dolomite, which occurs at ca. 740 °C, however dolomite has not been detected by XRD. On the other hand, small amount of dolomite, and its poor crystallinity could restrain its recognition by means of XRD analysis. This thermal effect could result from the presence of magnesian calcite, which decomposes at around 700 °C [26]. This interpretation is consistent with chemical data, which revealed presence of MgO in acid soluble fraction of the samples.

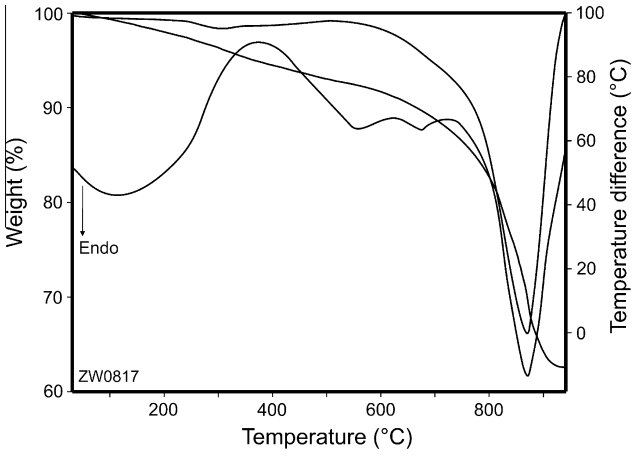

Fig. 11. DTA/TG/DTG curves of particle size fraction <0.063 mm from the primer plaster (sample ZW0817).

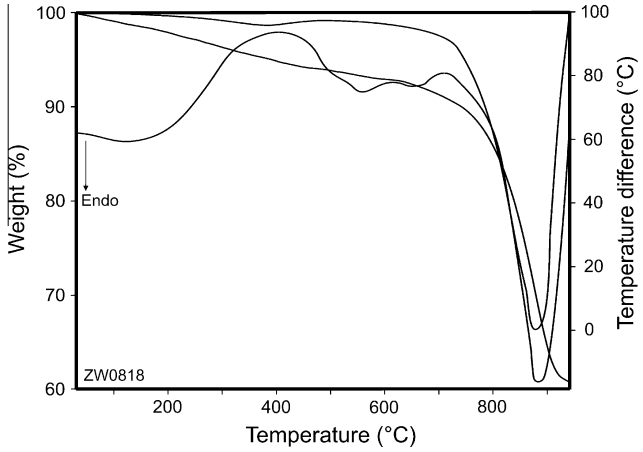

Fig. 12. DTA/TG/DTG curves of particle size fraction <0.063 mm from the sgraffito plaster (sample ZW0818).

Biotite or most likely hydrobiotite, whose presence is confirmed by OM observation as well as XRD analysis, is considered responsible for minor thermal effect, displayed as a small endothermic peak in the region of 200 °C (Figs. 11 and 12). Particularly hydrobiotite tends to loss zeolitic water and bonded water, process which undergoes in the temperature range 180–240 °C. Gypsum also decomposes below 200 °C, however no doublet at about 160 °C and 180 °C was observed, as well as significant weight loss. Although the SEM/EDAX analysis confirmed the presence of gypsum plates, this phase occurs in small quantity, below detection limit of TG/DTG/DTA as well as XRD, within samples dominated with carbonates.

4. Conclusions

A thorough study on mineralogy and the physical and mechanical properties of materials taken from historic masonry buildings is of primary importance for their future restoration. It defines the necessity to assure complete compatibility between original material and restoration mortars. In the case of the sgraffito decoration from Bożnów, we successively combined the "in situ" non-destructive examinations with successive destructive tests, to fulfill this demand. The non-destructive tests revealed that before the conservation treatment, the sgraffito decoration was exfoliated from the wall in ca. 90%. Original plasters were very fragile and extremely cracked. Most of the micrite was removed out by rainwater originated from damaged roof gutter, which mostly contributed to plasters disintegration. The shape of decoration could only be identified by differentiation between the rough surface of the scratched areas in contrast with relatively smooth parts once covered with lime paint. The acquired information, that fully documents the inner structure of the sgraffito decoration, allowed us to select the most adequate sampling areas for destructive tests.

The results of the mineralogical studies concerning the primer plaster and the sgraffito plaster lead to the conclusions that both layers results from similar production technologies. It is evidenced by comparable siliceous aggregate, showing related bimodal grain-size

distribution, and similar binder type. The primer plaster as well as the sgraffito plaster were a mixture of lime binder (aerial lime) and ordinary sand, compatible with local deposits of a material left by Pleistocene glacial meltwater streams. Additionally, the primer plaster contained small amount of brick chunks and charcoal, while the sgraffito plaster was strongly enriched in the latter. The role of charcoal was not limited to coloring agent. Porous charcoal chunks improved the permeability of the sgraffito plaster, which considerably contributed to a higher carbonation rate. The existence of hydraulic compounds was not evidenced, despite the presence of brick chunks. It is well known that the use of powdered bricks and tiles (i.e. artificial pozzolana) increases the hydraulicity of the lime mortars. However, pozzolanic effect is limited only to very finely powdered material, since it exclusively provides a large surface contact between the artificial pozzolana and lime, allowing for extensive reaction. Therefore, relatively large chunks observed within investigated mortars presumably served as aggregate, contrarily to the pozzolanic contribution. Small amounts of gypsum occur within the sgraffito plaster only. It should be regarded as a result of the reaction of atmospheric SO_x pollutant with carbonates from the topmost part of the decoration, which was directly exposed to the atmosphere. This phase also might contribute the degradation of the decoration due to the expansion during its crystallization.

The mineralogical analysis has revealed the composition, porosity, water absorption and hygroscopic properties of original plasters as well as the contents of water soluble salts. The results allow to choose the materials similar to the original ones, adequate for elimination of plaster exfoliation and resistant to the temperature and humidity changes characteristic for the climate in Poland. The non-destructive studies performed after conservation allowed to asses the efficiency of plaster consolidation as well as they prove that the rehabilitation work serves for the high efficiency of consolidation treatment by reestablishing the homogeneous structure of plasters.

The methodology described in this paper, involving non-destructive tests combined with destructive tests, demonstrates good accuracy in renovation practices of historic masonry.

Acknowledgements

The present study was supported by Grant no. 2022/W/ING/07-4. The authors wish to thank Prof. Jacek Puziewicz (University of Wrocław) for his valuable comments.

References

[1] Arıoglu N, Acun S. A research about a method for restoration of traditional lime mortars and plasters: a staging system approach. Build Environ 2006;41:1223–30.
[2] Grinzato E, Bison P, Marinetti S, Vavilov V. Nondestructive evaluation of delaminations in fresco plaster using transient infrared thermography. Res Nondestruc Eval 1994;5:257–74.
[3] Rosina E, Ludwig N, Torre SD, D'Ascola S, Sotgia C, Cornale P. Thermal and hygroscopic characteristics of restored plasters with different surface textures. Mater Eval 1994;66:1271–8.
[4] Daniels David J, editor. Ground penetrating radar. London: The Institution of Electrical Engineers; 2004.
[5] Middendorf B, Baronio G, Callebaut K, Hughes JJ. Chemical-mineralogical and physical-mechanical investigations of old mortars. In: Proceedings of the international RILEM-workshop "Historic mortars: characteristics and tests", Paisley; 2000. p. 53–61.
[6] Elsen J. Microscopy of historic mortars—a review. Cem Concr Res 2006;36:1416–24.
[7] Alvarez JI, Martín A, García Casado PJ, Navarro I, Zornoza A. Methodology and validation of a hot hydrochloric acid attack for the characterization of ancient mortars. Cem Concr Res 1999;29:1061–5.
[8] Bakolas A, Biscontin G, Contardi V, Franceschi E, Moropoulou A, Palazzi D, et al. Thermoanalytical research on traditional mortars in Venice. Thermochim Acta 1995;269(/270):817–28.
[9] Moropoulou A, Bakolas A, Bisbikou K. Investigation of the technology of historic mortars. J Cult Herit 2000;1:45–58.
[10] Maravelaki-Kalaitzaki Bakolas A, Moropoulou A. Physico-chemical study of cretan ancient mortars. Cem Concr Res 2003;33:651–61.
[11] Derric MR, Stulik D, Landry JM. Infrared spectroscopy in conservation science. Los Angeles: The Getty Conservation Institute; 1999.
[12] Moropoulou A, Bakolas A, Bisbikou K. Characterization of ancient, byzantine and later historic mortars by thermal and X-ray diffraction techniques. Thermochim Acta 1995;269(/270):779–95.
[13] Zappia G, Sabbioni C, Pauri MG, Gobbi G. Mortar damage due to airborne sulfur compounds in a simulation chamber. Mater Struct 1994;27:469–73.
[14] Martinez-Ramirez S, Puertas F, Blanco-Varela MT, Thompson GE. Studies on degradation of lime mortars in atmospheric simulation chambers. Cem Concr Res 1997;27:777–84.
[15] Franzini M, Leoni L, Lezzerini M, Sartoti F. On the binder of some ancient mortars. Mineral Petrol 1999;67:59–69.
[16] Zamba IC, Stamatakis MG, Cooper FA, Themelis PG, Zambas CG. Characterization of mortars used for the construction of Saithidai Heroon Podium (1st century AD) in ancient Messene, Peloponnesus, Greece. Mater Charact 2007;58:1229–39.
[17] Elsen J, Brutsaert A, Deckers M, Brulet R. Microscopical study of ancient mortars from Tournai (Belgium). Mater Charact 2004;53:289–94.
[18] Böke H, Çizera Ö, İpekoğlua B, Uğurlua E, Şerifakia K, Toprak G. Characteristics of lime produced from limestone containing diatoms. Constr Build Mater 2007;22:866–74.
[19] Degryse P, Elsen J, Waelkens M. Study of ancient mortars from Sagalassos (Turkey) in view of their conservation. Cem Concr Res 2002;32:1457–63.
[20] Sánchez-Moral S, Luque L, Cañaveras JC, Soler V, Garcia-Guinea J, Aparicio A. Lime pozzolana mortars in Roman catacombs: composition, structures and restoration. Cem Concr Res 2005;35:1555–65.
[21] Pavía S, Caro S. An investigation of Roman mortar technology through the petrographic analysis of archaeological material. Constr Build Mater 2008;22:1807–11.
[22] Boynton RS. Chemistry and technology of lime and limestone. New York: Wiley; 1980.
[23] Mertens G, Elsen J, Brutsaert A, Deckers M, Brulet R. Physical and chemical evolution of lime mortars from Tournai (Belgium). In: International building lime symposium, Orlando, Florida; 2005.
[24] Marques SF, Ribeiro RA, Silva LM, Ferreira VM, Labrincha JA. Study of rehabilitation mortars: construction of a knowledge correlation matrix. Cem Concr Res 2006;36:1894–902.
[25] Alvarez JI, Navarro I, García Casado PJ. Thermal, mineralogical and chemical studies of the mortars used in the cathedral of Pamplona (Spain). Thermochim Acta 2000;365:177–87.
[26] Bruno P, Calabrese D, Di Pierro M, Genga A, Laganara C, Manigrassi DAP, et al. Chemical–physical and mineralogical investigation on ancient mortars from the archaeological site of Monte Sannace (Bari—Southern Italy). Thermochim Acta 2004;418:131–41.